Feasibility of Guided-Wave Optical Microphone Based on Elasto-Optic Effect

Hiroyuki Nikkuni[a], Masashi Ohkawa*[b], Seishi Sekine[b], and Takashi Sato[b]
[a] Graduate School of Science and Technology, Niigata University
8050 Ikarashi 2-no-cho, Niigata 950-2181, Japan
[b] Faculty of Engineering, Niigata University
8050 Ikarashi 2-no-cho, Niigata 950-2181, Japan

ABSTRACT

In this paper, the feasibility of a glass-based guided-wave optical microphone is described. The optical microphone consists of a rectangular diaphragm and a straight waveguide on the diaphragm. The sensitivity of the microphone and the resonance frequency of the diaphragm are dependent on the diaphragm dimensions. In this study, to confirm operation of the proposed optical microphone, the target values for phase sensitivity and resonance frequency were set at 1.3 mrad/Pa and 5 kHz, respectively. By design considerations, the diaphragm dimensions were determined to be 16 mm× 16 mm× 0.15 mm. After fabrication, a sound wave of 1 kHz and 25 Pa, corresponding to 122 dB-SPL (sound pressure level), was applied to the microphone. In the experiment, the intensity-modulated output with the same frequency as the applied sound wave was obtained, but the observed output was unexpectedly caused by misalignment of the optical components due to mechanical vibration. The estimated output signal by the normal operation of the microphone for a sound pressure of 25 Pa was 1/10 - 1/100 of the noise level, according to the measured output characteristic to static pressure. In order to detect normal speech ranging from 55 to 65 dB-SPL, the S/N ratio should be improved by a factor of more than 10^4.

Keywords: optical microphone, guided-wave optics, glass, diaphragm, elasto-optic effect

1. INTRODUCTION

In Magnetic Resonance Imaging (MRI), microphones are useful tools in patient-to-physician and physician-to-physician communications. Since strong magnetic fields are produced in the MRI scanner during operation, conventional dynamic microphones, which are based on the electromagnetic effect, cannot be used in the scanner room. Also, condenser and electret microphones, as well as dynamic microphones, contain metal parts that would damage the MR image, and therefore cannot be used in MRI communications either. Using lightwave sensing technology can overcome serious obstacles related to conventional microphones in MRIs because the optical system is not affected by electromagnetic interference and requires no metal parts. Our group is developing silicon-based and glass-based guided-wave optical microphones[1], based on the guided-wave optical pressure sensors[2-5], which do not rely on any electromagnetic effect or contain any metal parts. So, the optical microphones can be used even in a hazardous environment, such as in a high magnetic field like the MRI, high RFI fields, and other environments that require EMI/RFI immunity. In our previous work, the fabricated guided-wave optical microphone had a rather low S/N ratio, so a lock-in amplifier was used to detect output signal. The output signal, which was proportional to sound pressure, was obtained successfully, but the lock-in detection is not practical for microphones. In this study, the feasibility of guided-wave optical microphone was examined without the lock-in detection by increasing sensitivity. The fabricated microphone had a diaphragm of 16 mm×16 mm×0.15 mm, and its measured phase sensitivity was 0.90 mrad/Pa, which is 7.5 times higher than that in the previous report[1]. In the experiment, a sound wave of 25 Pa and 1 kHz was applied to the fabricated optical microphone using a loudspeaker. The output signal by normal operation of the microphone was not observed since it was disturbed by the misalignment of the optical components which vibrated by the applied sound. However, from the estimated output signal and the observed noise, the minimum detectable sound pressure level of the fabricated microphone was estimated to be 140 dB-SPL or higher. Since normal speech ranges from 55 to 65 dB-SPL, it was determined that improvement of the S/N ratio by at least a factor of 10^4 is required to detect normal speech. There is ample room for reduction of noise and to increase sensitivity, so the use of a guided-wave optical microphone in a harsh environment is still promising.

Optomechatronic Sensors and Instrumentation, edited by Yasuhiro Takaya, Proc. of SPIE Vol. 6049, 604907, (2005)
0277-786X/05/$15 · doi: 10.1117/12.649176

2. PRINCIPLES OF OPERATION

Figure 1 shows a glass-based guided-wave optical microphone. The microphone has a rectangular diaphragm as a pressure-sensitive mechanical structure and a single-mode optical waveguide across the diaphragm. A plate with a small hole is attached to the microphone to shield the bottom face of the diaphragm from diffracted sound waves, so that only the top face of the diaphragm is exposed to sound pressure. A small hole is provided to avoid any influence caused by fluctuations of the atmospheric pressure, by connecting the closed space under the diaphragm and the ambient atmosphere. An optical microphone is placed between a pair of crossed polarizers, as shown in Fig. 1. The input polarizer is oriented at 45° with respect to the polarization of each guided mode. The light beam from the input polarizer is coupled to the fundamental TM-like and TE-like modes at equal intensities. When a sound wave is applied to the diaphragm, the diaphragm is distorted by vibration. The distortion causes strain, which produces a change in the refractive index of the diaphragm by the elasto-optic effect. The index change produces phase retardation in the lightwave, which propagates in the waveguide on the diaphragm. Phase retardation is dependent on the guided modes, and phase difference between the two modes is also a function of the applied pressure. The lightwave has linear, elliptic or circular polarization at the end of the waveguide corresponding to the induced phase difference. The crossed output polarizer converts the polarization-modulated light into intensity-modulated light. The power of the beam passing through the output polarizer changes with the magnitude of sound pressure.

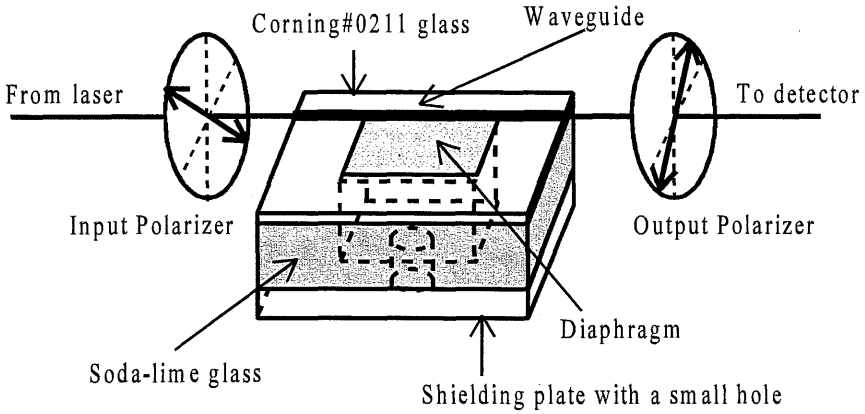

Fig. 1 Schematic diagram of a guided-wave optical microphone placed between a pair of crossed polarizers.

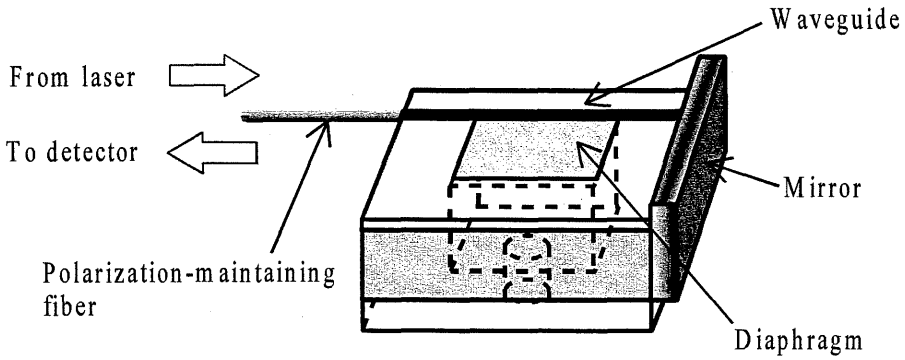

Fig. 2 Schematic drawing of a realistic glass-based guided-wave optical microphone.

Incidentally, the optical microphone shown in Fig.1 has a practical difficulty since oversized polarizers and objects are used and precise alignment is required to couple the lightwave to the guided waves. Figure 2 shows a schematic drawing

of a realistic guided-wave optical microphone. The polarization-maintaining fiber, which is substituted for the polarizers, is connected to one endface of the microphone, and a mirror is attached to the other endface. The lightwave from the laser is sent to the optical microphone by the fiber. Then, the lightwave modulated on the diaphragm reflects back to the fiber by the end mirror.

3. THEORY FOR DESIGN OF THE MICROPHONE

3.1. Phase sensitivity of the microphone

Sensitivity is an important factor to determine the characteristics of the guided-wave optical microphone. Phase sensitivity, defined as the induced phase difference per unit pressure, is known to be dependent on the dimensions of the diaphragm.[4, 5] In this subsection, numerical formulas to calculate sensitivity versus diaphragm dimensions are described.[3] It is assumed that the rectangular diaphragm has an area of $a \times b$ and a thickness of h, and all edges of the diaphragm are rigidly clamped. Regarding the coordinate axis, the y-z plane lies in the middle plane between the two surfaces of the diaphragm, and the z-axis is parallel to the waveguide. The x-axis is perpendicular to the plate surface.
Deflection w of the diaphragm, or displacement from equilibrium, due to uniformly applied pressure q, is obtained from the following differential equation:[3, 6]

$$\frac{\partial^4 w}{\partial y^4} + 2\frac{\partial^4 w}{\partial y^2 \partial z^2} + \frac{\partial^4 w}{\partial z^4} = \frac{q}{D}, \tag{1}$$

where D is flexural rigidity, defined as $D = Yh^3/12(1-\mu^2)$. Also, Y and μ are the modulus of elasticity and the Poisson's ratio, respectively. From the obtained deflection, the distribution of stress in the diaphragm is derived.[3] Next, the strain distribution S is calculated from stress distribution, assuming that Hooke's law applies.[3] The anisotropic refractive index change Δn due to the induced strain is given by

$$\Delta n_i = -\frac{1}{2} n^3 p_{ij} S_j \qquad (i, j = 1 - 6), \tag{2}$$

where n is the refractive index of the diaphragm, and p_{ij} denotes each component of the elasto-optic tensor. The strain has six components, which are divided in two kinds of strain: normal strains in the x, y and z directions with subscripts 1, 2 and 3 respectively, and shearing strains with subscripts 4, 5 and 6. The index changes, Δn_1 and Δn_2, give different phase retardations to the two guided waves traveling on the diaphragm. The amount of phase difference $\Delta\phi$ between them is expressed as

$$\Delta\phi = \Delta\phi_{\mathrm{TM}} - \Delta\phi_{\mathrm{TE}}, \tag{3}$$

where

$$\Delta\phi_{\mathrm{TM}} \approx \int_{-b/2}^{b/2} \left(\frac{\omega\varepsilon_0 n}{2} \int_{-a/2}^{a/2} \int_{-h/2}^{h/2} E_x(x,y) \Delta n_1(x,y,z) E_x^*(x,y) dx dy \right) dz, \tag{4}$$

and

$$\Delta\phi_{\mathrm{TE}} = \int_{-b/2}^{b/2} \left(\frac{\omega\varepsilon_0 n}{2} \int_{-a/2}^{a/2} \int_{-h/2}^{h/2} E_y(x,y) \Delta n_2(x,y,z) E_y^*(x,y) dx dy \right) dz, \tag{5}$$

where ω is the angular frequency of the light, ε_0 is the permittivity of the vacuum, and * indicates complex conjugate. Also, E_x and E_y are the power-normalized x-directed electric field component of the TM-like mode and the power-normalized y-directed electric field component of the TE-like mode, respectively. In this study, phase sensitivity, defined as the resultant phase difference calculated by eq. (3) per unit pressure, is used as microphone sensitivity.
According to the theoretical calculations, the phase sensitivity is proportional to the cube of the shorter or longer side length, and also inversely proportional to the square of the diaphragm thickness.

3.2 Resonance frequency of the diaphragm

Figure 3 shows the frequency response of the optical microphone. The upper boundary of the frequency range must be sufficiently lower than the resonance frequency. To widen the frequency range, the resonance frequency should be set higher. The resonance frequency is derived from the following differential equation for free vibration of the diaphragm.

$$\rho h\frac{\partial^2 w}{\partial t^2}+\frac{Yh^3}{12(1-\mu^2)}\left(\frac{\partial^4 w}{\partial y^4}+2\frac{\partial^4 w}{\partial y^2\partial z^2}+\frac{\partial^4 w}{\partial z^4}\right)=0, \tag{6}$$

where ρ is the density of the diaphragm. The resonance frequency is dependent on diaphragm dimensions and a support condition of the diaphragm edge. In case of a square diaphragm with the side length of a, the resonance frequency is known as

$$f=\frac{3.646\pi}{2}\sqrt{\frac{Y}{12\rho(1-\mu^2)}}\frac{h}{a^2}, \tag{7}$$

under the assumption that all the edges are rigidly clamped. It is found from eq. (7) that the resonance frequency is proportional to the thickness of the diaphragm, and also inversely proportional to the square of the side length.

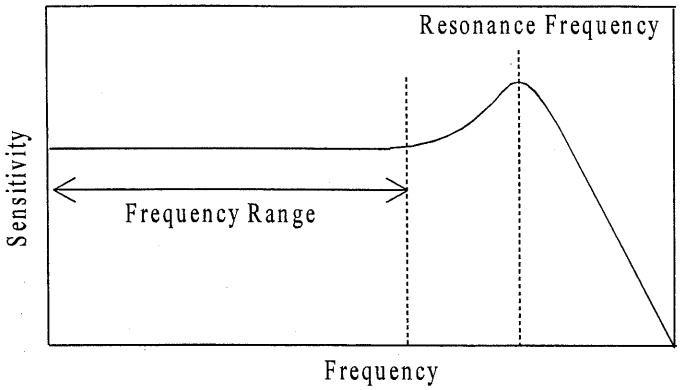

Fig. 3 Frequency response of the optical microphone.

3.3 Designing of the guided-wave optical microphone

Phase sensitivity and resonance frequency were calculated from eqs. (3) and (7) in order to make the chart shown in Fig. 4 for the design of the guided-wave optical microphone. In the calculation, the edge of the diaphragm was chosen as a waveguide position, where sensitivity is the highest. The wavelength of the guided light was also set at 633 nm. Moreover, we used the mechanical and optical parameters of Corning #0211 glass, of which the diaphragm was made, except for the elasto-optic coefficients of fused silica. The coefficients of fused silica are similar to those of glass, so this does not affect the theoretical results. In Fig. 4, the calculated trajectories of equal sensitivities are shown with solid lines on the side length - thickness plane. Since the sensitivity of the microphone is proportional to a^3 / h^2, the slopes for the sensitivities are 1.5 in Fig. 4. Also, calculated trajectories of equal resonance frequency are shown with dashed lines in Fig. 4. Since resonance frequency of the diaphragm is proportional to h / a^2 from eq. (7), the slope for the resonance frequency is 2 in Fig. 4.

From Fig. 4, sensitivity is found to increase as the side length of the diaphragm lengthens, while resonance frequency decreases. Also, sensitivity increases as thickness thins, while resonance frequency decreases. Since it is difficult to realize both higher sensitivity and higher resonance frequency, one of these conditions may need to be sacrificed in order to satisfy the other when designing the guided-wave optical microphone. In this study, the target values of sensitivity and resonance frequency were set at 1.3 mrad/Pa and 5 kHz, respectively. Since the main concern of this study was placed on sensitivity rather than resonance frequency, a resonance frequency of 5 kHz is not necessarily appropriate for practical uses, even for bandwidth-limited telecommunication. From Fig. 4, the diaphragm dimensions were determined to be 16 mm× 16 mm× 0.15 mm.

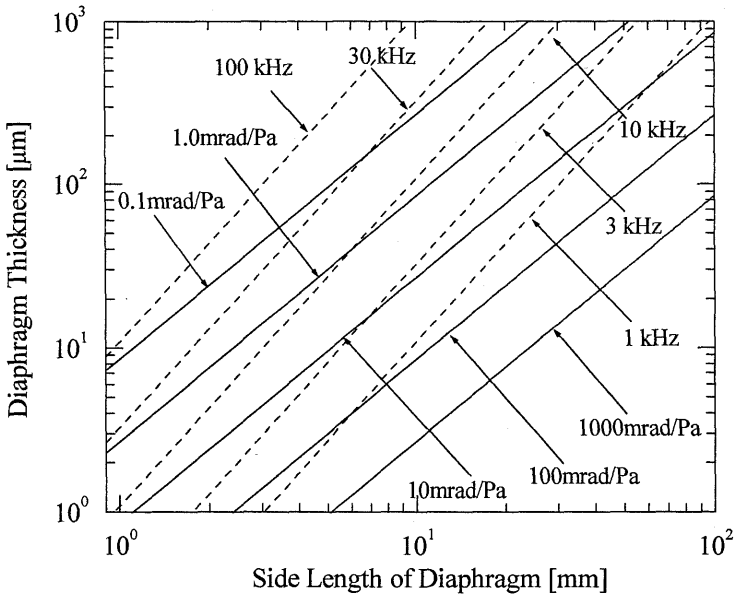

Fig. 4 Theoretical trajectories of equal sensitivities and equal resonance frequencies on the side length - thickness plane.

4. EXPERIMENT

4.1. Fabrication

Figure 5 shows a schematic diagram of the fabricated optical microphone according to actual dimensions. The microphone was built using two glasses: a Corning #0211 glass as a diaphragm plate and a soda-lime glass with a 16 mm×16 mm square hole to support the diaphragm plate. First, a thin aluminum film was evaporated on a Corning glass 0.15 mm thick. The aluminum film was removed by using a patterned photoresist as a mask. Then, the glass was immersed in KNO_3 for two hours at 400℃ to form the single-mode channel waveguides. The waveguide was adjusted to be parallel to the diaphragm, and then the two substrates were bonded together by UV adhesion. Finally, a shielding plate with a small hole was attached to the microphone to shield the bottom of the diaphragm from diffracted sounds.

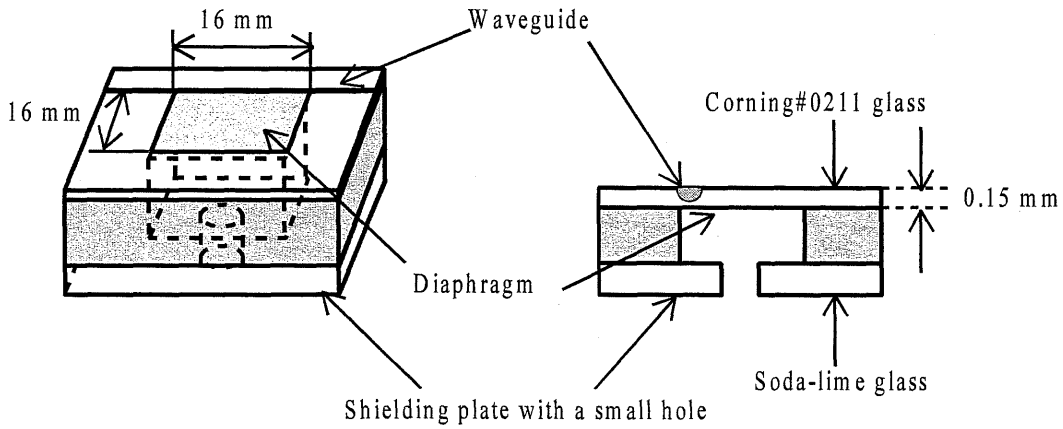

Fig. 5 Schematic drawing of the fabricated optical microphone.

4.2. Output characteristic of optical microphone to static pressure

Figure 6 illustrates the experimental setup used to evaluate the phase sensitivity of the microphone from the output characteristic to static pressure. Pressure was applied to the diaphragm by connecting a 3 ml syringe to the microphone with a silicone tube. Pulling and pushing the plunger of th e syringe caused pressure difference, ranging from –5.7 kPa to 6.5 kPa, on the diaphragm. A positive value represents pressure in the closed space being higher than that in the atmosphere. A linearly-polarized He-Ne laser at 633 nm was used as the light source. Its polarization was set at 45° with respect to the microphone surface, so that an input polarizer as shown in Fig. 1 was not necessary. Moreover, output light from the microphone was passed through a pinhole to block stray light. Output power was detected by a conventional photodiode.

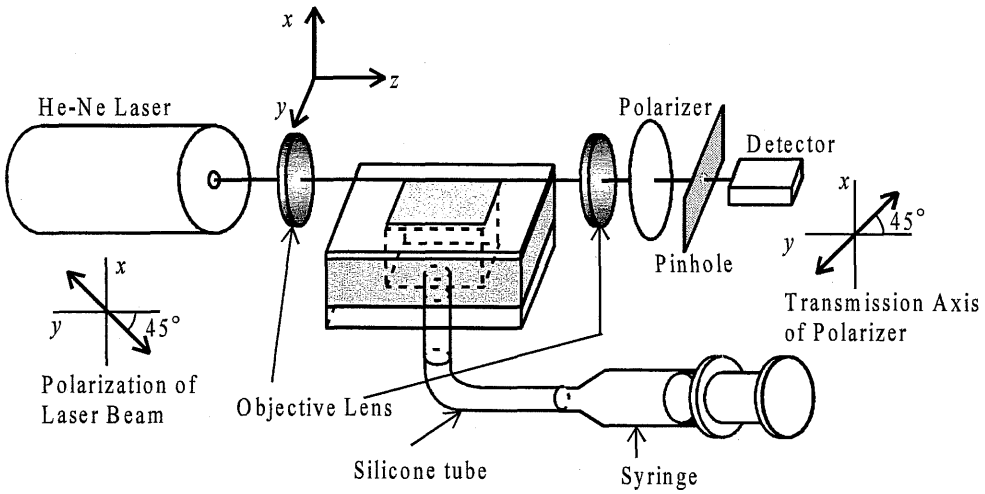

Fig. 6 Experimental setup used to evaluate phase sensitivity.

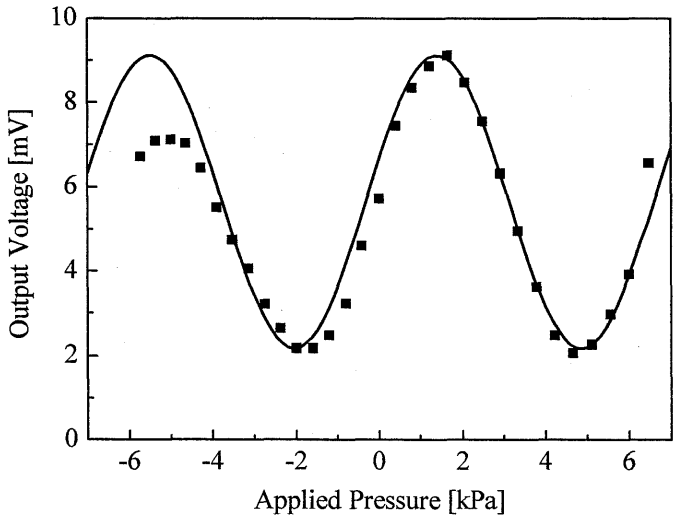

Fig. 7 Output voltage from the detector versus applied pressure.

Figure 7 shows the experimental results. The solid line in the figure indicates the computer prediction of the experimental data. The output power sinusoidally changes with the applied pressure. A half period of the output power is called the halfwave pressure, which corresponds to a phase difference of π rad. From Fig. 7, the halfwave pressure was evaluated to be 3.5 kPa, corresponding to a phase sensitivity of 0.90 mrad/Pa. The measured sensitivity was 70% of the

theoretical prediction. This difference was attributed to a relaxation of induced strain near the diaphragm edge. The relaxation was caused mainly by imperfect bonding by UV adhesion, which reduced the rigidity of the support structure surrounding the diaphragm.

4.3. Output response of optical microphone to sound wave

Figure 8 shows the experimental setup used to detect output power in response to a sound wave. The output signal was observed with an oscilloscope while a sound wave of 25 Pa and 1 kHz was applied to the fabricated microphone. A loudspeaker with a diameter of 80 mm was used as the sound source. To reduce mechanical vibration of the optical system due to the loudspeaker, the loudspeaker was isolated from the optical table by hanging it with wires above the fabricated optical microphone. Moreover, sound pressure was calibrated by a condenser microphone with a known sensitivity.

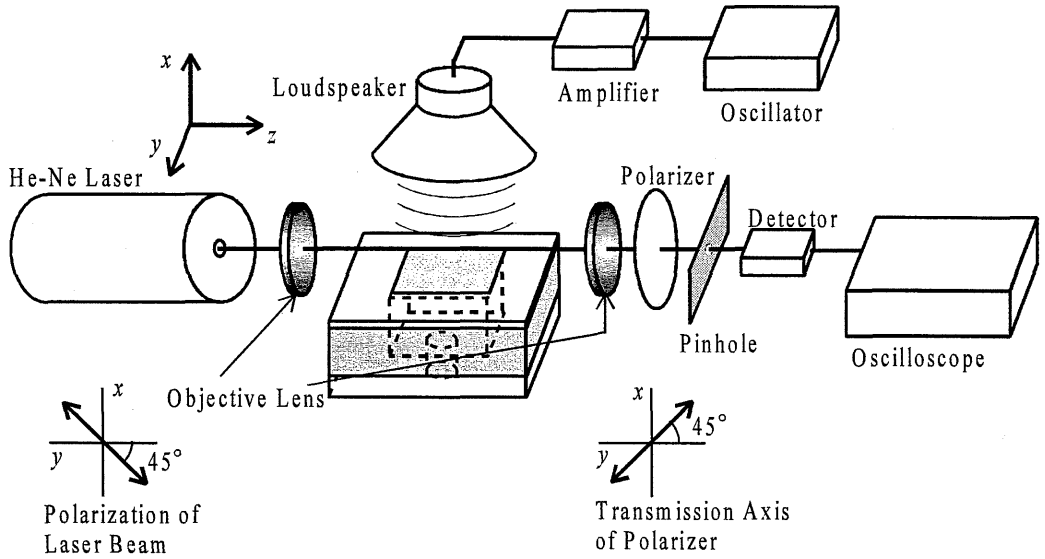

Fig. 8 Experimental setup to measure output power in response to sound wave.

Figure 9 shows a photograph of the output signal responding to a sound wave of 25 Pa and 1 kHz. This response was obtained for the waveguide position nearest to the diaphragm edge where the sensitivity is at maximum. The intensity-modulated output with the same frequency as the applied sound wave was observed although amplitudes of the output signal and noise are almost same, less than 1 mV. Incidentally, from Fig. 7, the tangential slope is 2.9 mV/kPa around 0 kPa, which is the operating point of the microphone. From the tangential slope of 2.9 mV/kPa, the output voltage is estimated to be only 73 μV at most for a sound pressure of 25Pa. The estimated output voltage was much less than the measured one, in the order of hundreds of millivolts, and was 1/10 - 1/100 of the noise level. In order to determine whether the observed output signal was produced under normal operation of the microphone, the same experiment was done for the waveguide placed at 2 mm off from the diaphragm edge where no output signal is expected. Unfortunately, an output signal was observed even for the waveguide outside the diaphragm. This means that the observed output signal did not result from normal operation of the microphone. The signal may have been caused by the misalignment of the optical components, especially the fabricated microphone, by mechanical vibration.

The applied sound pressure of 25 Pa corresponds to a sound pressure level of 122 dB-SPL, which slightly exceeds the discomfort threshold for people with normal hearing. From the estimated signal level and the observed noise level, the minimum detectable sound pressure level of the microphone is estimated to be 140 dB-SPL or higher. The optical microphone should be able to detect normal speech ranging from 55 to 65 dB-SPL by improving the S/N ratio by a factor of more than 10^4. Such an improvement is possible since there is still room for reduction of noise and an increase in sensitivity by a factor of 10^2 each.

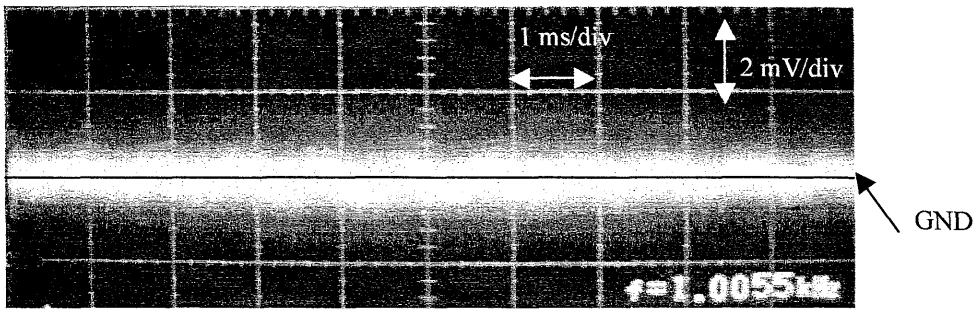

Fig. 9 A photograph of output signal responding to a sound wave of 25 Pa and 1 kHz.

5. CONCLUSIONS

We have developed a guided-wave optical microphone based on the elasto-optic effect. In the experiment, an output signal with the same frequency as the applied sound wave was observed, but the signal was not due to normal operation of the microphone but due to misalignment of the optical components by mechanical vibration. To maintain alignment, the optical fiber should be connected to one endface of the microphone as shown in Fig. 2. Moreover, the minimum detectable sound pressure level of the fabricated microphone was estimated to be 140 dB-SPL or higher, so the S/N ratio of the microphone needs to be improved by a factor of more than 10^4 in order to detect normal speech. In order to increase in output signal, the diaphragm area should be increased as well as the diaphragm thickness be decreased. Regarding the decrease in noise, since no countermeasures for noise were taken in this study, large noise reduction can be expected by using a band pass filter that allows the properly chosen frequency band to pass.

ACKNOWLEDGMENTS

This work is supported in part by a Grant-in-Aid for Scientific Research (No.17360157) from the Japan Society for the Promotion of Science.

REFERENCES

1. H. Nikkuni, S. Dokko, M. Ohkawa, S. Sekine, and T. Sato: "Optical microphone using a silicon-based guided-wave optical pressure sensor," Proc. SPIE, **5728**, pp. 317-324, 2005.
2. M. Ohkawa, Y. Shirai, T. Goto, S. Sekine, and T. Sato: "Silicon-based integrated optic sensor using intermodal interference between TM-like and TE-like modes," Fiber and Integrated Optics, **21**, pp.105-113, 2002.
3. M. Ohkawa, K. Hasebe, S. Sekine, and T. Sato, "Relationship between Sensitivity and Waveguide Position on the Diaphragm in Integrated Optic Pressure Sensors Based on the Elasto-Optic Effect," Appl. Opt., **41**, pp.5016-5021, 2002.
4. A. Yamada, T. Tokita, M. Ohkawa, S. Sekine, and T. Sato, "Scale reduction rule for diaphragm dimensions to miniaturize a silicon-based integrated optic pressure sensor without reducing sensitivity," Proc. SPIE, **4987**, pp. 248-255, 2003.
5. Y. Iwase, Y. Okamoto, M. Ohkawa, S. Sekine, and T. Sato, "Sensitivity dependence with respect to diaphragm dimensions in a glass based integrated optic pressure sensor," Proc. SPIE, **4987**, pp. 256-263, 2003.
6. S. P. Timoshenko and S. Woinowsky-Krieger, *Theory of Plates and Shells* , McGraw-Hill Kogakusha, Tokyo, 1981.

* Correspondence: E-mail: ohkawa@eng.niigata-u.ac.jp; Telephone & FAX: +81-25-262-6734